Journal of Sciences, Islamic Republic of Iran 21(4): 321-331 (2010) http://jsciences.ut.ac.ir
University of Tehran, ISSN 1016-1104

An Investigation on the Composition of Biotite from Mashhad Granitoids, NE Iran

A.A.T. Shabani,[1,*] F. Masoudi,[2] and F. Tecce[3]

[1] *Research Center for Earth Sciences, Geological Survey of Iran, Tehran, Islamic Republic of Iran*
[2] *Faculty of Earth Sciences, Shahid Beheshti University, Tehran, Islamic Republic of Iran*
[3] *Istituto Geologia Ambientale e Geoingegneria, C.N.R., Rome, Italy*

Received: 31 July 2010 / Revised: 31 October 2010 / Accepted: 16 November 2010

Abstract

Compositions of biotite from three different rock types of Mashhad granitoids, i.e., granodiorite, monzogranite and leucogranite in NE of Iran have been documented by electron microprobe and wet chemistry for Fe^{3+} and Fe^{2+}. Mashhad granitoids have been geochronologically and petrologically grouped into G1 and G2 phases. Microprobe data show that the total Fe contents in biotite from G2 leucogranite are higher than those in biotite from G1 granites. In addition, the oxidation state of iron determined by wet chemistry shows that $Fe^{3+}/(Fe^{2+} + Fe^{3+})$ ratio in biotite from G2 leucogranite is 0.10 indicating relatively reducing whereas, in G1 ones is 0.18 and 0.23 suggesting more oxidizing conditions. The most outstanding compositional characteristics of Mashhad biotite are differences in total Al contents and Fe/(Fe+Mg) ratios. In the annite-siderophylite-phlogopite-eastonite (ASPE) quadrilateral, represented based on the above parameters, biotite samples from G1 and G2 granites define two distinct and non-overlapping trends. Each trend is characterized by a pronounced trend of increasing total Al at relatively narrow Fe/(Fe+Mg) values. The total Al contents of G1 biotite are in the range of 2.8 to 3.1, whereas, in G2, 3.3 to 3.6 (apfu). Fe/(Fe+Mg) values of G1 biotite are in the range of 0.52 to 0.59 which is considerably lower than those from G2 biotite, 0.67 to 0.72. The trend of increasing Al contents at constant Fe/(Fe+Mg) is relatively common and observed in biotite from several locations worldwide and attributed to considerable contributions from aluminous supracrustal material, either by assimilation or anatexis.

Keywords: Biotite; Granitoids; Mashhad; Iran

Introduction

Biotite is a phyllosilicate mineral that can accommodate most of the common elements present in the granitic magmas, a feature which makes it a valuable probe of magma composition. Therefore, the use of biotite composition as a valuable tool to study granite petrogenesis has recently been shown by for

* Corresponding author, Tel.: +98(21)64592285, Fax: +98(21)66070517, E-mail: aatshabani@gmail.com

instance, Ague and Brimhall [2], Hecht, [20], Stone et al. [52], Sallet [45], Stone [53], Ghani [18], Jiang et al. [25], Aydin et al. [6], Li et al. [31], Shabani et al. [46], Kumar et al. [29], Buda et al. [11], Machev et al. [33], Lima et al. [32] and Bónová et al. [9].

Most recently, studies by Nachit et al. [38], Lalonde and Bernard [30], Burkhard [12], Abdel-Rahman [1], Shabani et al. [46], Bónová et al. [8], Barzegar [7], Masoudi and Jamshidi-Badr [36] and Esmaeily and Maghdour-Mashhour [16] have shown that biotite has also potential to be used as a tectonomagmatic indicator in granites. The basis for selecting biotite as a tectonomagmatic indicator is because this mineral is the most important host of any excess aluminum in granites that lack significant values of alumino-silicate polymorphs, garnet and cordierite; therefore, it reflects directly the peraluminosity of the host magma. In addition, it is also the most readily available indicator of oxidation state of the rock. Peraluminosity and relative oxidation state of the magma have been the basis for the classification of granites into I- and S-types [13] and ilmenite- and magnetite-series [23, 24], respectively.

The three major rock varieties of Mashhad granitoids are hornblende biotite tonalite – granodiorite, feldspar monzogranite and biotite – muscovite leucogranite [27]. The samples used for this study come from Gheshlagh and Khajehmourad areas, south east of Mashhad city. What primarily persuaded us to examine the composition of biotite, the main or sole ferromagnesian mineral in these rocks were the differences in its pleochroic colors, seen in plane polarized light.

Biotite in some of granodiorite samples is green; in monzogranite and other granodiorite samples is brown and in leucogranite samples is entirely reddish-brown. Therefore, the aim of this paper in particular is to document by electron microprobe the chemical composition of biotite from different rock types, explore its compositional characteristics, illuminate the petrogenesis and infer the possible tectonic environment.

Materials and Methods

Brief Regional Geologic Setting and Granitoid Plutonism

Binaloud zone in the north east of Iran, is located at the south and west of Mashhad city. This zone, located also between Turan plate and the Central Iran block (Fig. 1), is regarded as a part of remnant of Paleo-Tethys (meta-ophiolite and meta-flysch) intruded by granitic rocks during Triassic to Cretaceous periods [27]. It is believed that Binaloud zone with NW trend results from the collision of Turan plate with NE Central Iran plate at Late Triassic. Readers are referred for further detailed geology to for instance, Alavi, [3, 4]; Taheri and Ghaemi, [54]; Shahrabi, [48]; Hasanie pak et al., [19] and Karimpour et al., [27, 28].

The granitic rocks called "Mashhad granitoids" were intruded into Binaloud zone during Triassic to Cretaceous periods. The rocks have been studied by numerous authors (e.g., [5, 35, 42, 37, 56, 22, 15, 55, 27, and 28]). In the following for our purpose a very brief description of the geology of granitoids is presented.

Mashhad granitoids covers an outcrop area of 350 km^2 in the south east of Mashhad city (Fig. 1). The main rock types are tonalite – granodiorite, feldspar monzogranite and leucogranite cut by aplitic and pegmatitic veins. According to Majidi [35] the granitoids were formed as a result of three phases of magmatic activities in different time periods. The first phase called G1 granite (comprising tonalite – granodiorite and feldspar monzogranite) formed most likely in the Triassic period. The second phase called G2 granite (biotite – muscovite leucogranite) formed in the Jurassic and the third phase called G3, the latest phase cutting G1 and G2 granites, comprises aplitic granite and aplite-pegmatite veins. Feldspar monzogranite and leucogranite with a NW-SE trend comprise the main portion of the granitoids.

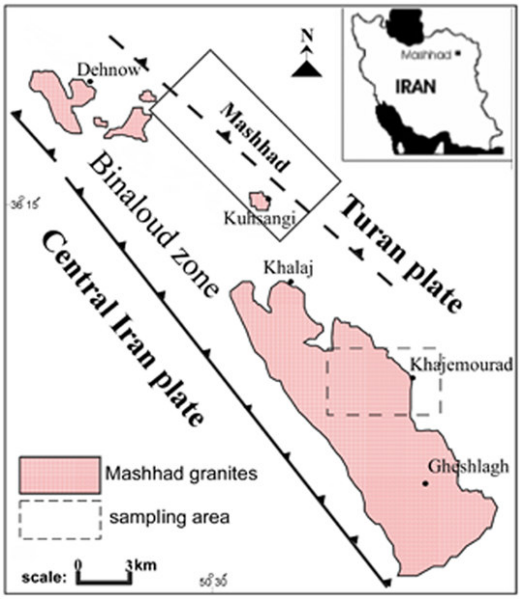

Figure 1. A simplified map showing structural zones in north east of Iran and the outcrop of Mashhad granitoids.

According to Karimpour et al., [27] tonalite and granodiorite are meta to moderately peraluminous I- to S-type calc-alkaline granites; feldspar monzogranite is moderately peraluminous, K-rich calc-alkaline type and biotite muscovite leucogranite is highly peraluminous S-type in terms of its enclaves, mineralogy (monazite, ilmenite and muscovite) and geochemical characteristics which is similar to those of syn-collision granites. The tonalite and granodiorite are considered to be originated from a mafic source; monzogranite from deeper source and contaminated by the crustal materials and biotite muscovite leucogranite from the continental crust.

Sample Selection

The granodiorite and monzogranite used in this study were collected from intrusive bodies cropped out in the south east portions of plutonic belt in Gheshlagh area and biotite muscovite leucogranite from Khajemourad area. A brief petrography description of each of the rock types is presented below based on their own distinct pleochroic colors of biotite.

The granodiorite samples (Tp-28, Tp-36), characterized by green pleochroic biotite, are medium to coarse grained, grey, moderately foliated granular, composed essentially of plagioclase, quartz (showing wavy extinction), ±large white alkali feldspar crystals exhibiting porphyritic texture, and biotite. Myrmekite occurs occasionally beside plagioclase crystals. Accessories include allanite, titanite, traces of magnetite, apatite, zircon, chlorite, and sericite.

The granodiorite and monzogranite samples (Tp-24, Tp-29, Tp-35 and Tp-41), characterized by brown pleochroic biotite, are medium to coarse grained grey moderately foliated granular, composed of plagioclase, ±large pink alkali feldspar crystals (giving these rocks a porphyritic texture), biotite and quartz (showing wavy extinction). Myrmekite can also be seen infrequently adjacent to plagioclase crystals. Minor constituents include secondary ±muscovite, ±allanite, ±titanite, apatite, zircon, chlorite, sericite and traces of ±magnetite.

The leucogranite samples (Tp-42, Tp-45, and Tp-23), characterized by reddish brown pleochroic biotite, are fresh unaltered non-foliated medium grained leucocratic granular, consists primarily of plagioclase, quartz, microcline, biotite and primary muscovite. Accessories include apatite, zircon, sericite and rare traces of ilmenite.

Electron Microprobe Analysis

Biotite analyses were obtained by wavelength-dispersive X-ray spectrometry on polished thin sections prepared from each rock sample described above for 12 elements using a Cameca SX-50 electron microprobe at the Istituto di Geologia e Geoingegneria Ambientale, C.N.R., University La Sapienza of Rome, Italy. Typical beam operating conditions were 15 kV and probe current 15 nA. The counting time for analysis of each element was 20 seconds except for F, 30 seconds. The accuracy of the analyses is 1% for major and 10% for minor elements. The standards used for the elemental analyses were as follow: synthetic fluorphlogopite for F, wollastonite for Si and Ca, corundum for Al, magnetite for Fe, periclase for Mg, rutile for Ti, sylvite for Cl, barite for Ba, pure Mn for Mn, orthoclase for K and jadeite for Na. Finally, matrix effects were corrected using the PAP Program provided by Pouchou and Pichoir [43]. Traverse Microprobe point analyses from rim to core and from core to rim showed no significant chemical variation indicating equilibrium crystallization for biotite. A total of 189 point analyses were collected. Note that the chemical composition of each with its respective structural formula based on 22 oxygen atoms can be obtained from the author upon request.

FeO and Fe_2O_3 Determination

Contents of FeO and Fe_2O_3 were determined for three different samples of biotite separates (Tp-42, Tp-24, and Tp-36) through wet chemistry in the chemistry laboratory of the Geological Survey of Iran. To separate mica from rock for ferrous and ferric iron determination, whole rock samples were crushed using both jaw crusher and pulverizer. The crushed samples were then sieved to obtain the size fraction between 45 and 60 mesh (350-250 μm). All samples were washed with water to remove dust. Magnetite was removed with a strong permanent magnet and the mafic and felsic grains were then separated using heavy liquids (methylene iodide, S.G. = 3.33). Final shaking on a tilted paper sheet and hand-picking were performed for all samples until the biotite concentrates appeared at least 99% pure under the binocular microscope. Then to prevent contamination and oxidation of ferrous iron, the biotite grains were ground under acetone in an agate mortar and pestle to obtain a fine powdered sample. Powdered mica dissolves more readily during acid attack than the granular micas and thus yields higher precision and accuracy of ferrous and ferric iron determinations [47].

Whole-Rock XRF Analyses

Whole-rock major, minor and trace elements were

Table 1. XRF rock analyses of different types of Mashhad G1 and G2 granites along with their CIPW normative minerals. Oxides in wt.% and trace elements in ppm

	G1 granites						G2 granites		
Oxides %	Tp-28	Tp-36	Tp-24	Tp-35	Tp-41	Tp-29	Tp-45	Tp-42	Tp-23
SiO_2	63.32	66.46	64.91	68.10	71.59	63.39	72.05	72.44	70.67
TiO_2	0.56	0.41	0.65	0.41	0.32	0.82	0.22	0.18	0.27
Al_2O_3	16.28	16.53	15.56	15.90	14.52	15.84	14.97	14.89	16.07
Fe_2O_{3tot}	4.10	3.30	4.43	2.77	2.33	5.44	1.73	1.52	1.64
MnO	0.10	0.08	0.09	0.07	0.05	0.14	0.05	0.04	0.03
MgO	2.64	1.15	1.60	1.07	0.65	2.08	0.34	0.30	0.41
CaO	3.82	2.51	3.71	2.31	2.06	4.37	1.26	1.16	1.08
Na_2O	4.01	3.95	3.73	3.50	3.60	3.67	4.04	3.42	3.18
K_2O	3.95	3.91	3.16	4.67	3.72	2.29	4.21	4.50	5.51
P_2O_5	0.36	0.30	0.53	0.25	0.15	0.67	0.14	0.15	0.13
Total	99.14	98.60	98.37	99.05	98.99	98.71	99.01	98.60	98.99
Trace elements (ppm)									
Sc	9	8	10	6	7	14	1	5	5
V	58	44	63	37	29	92	9	10	15
Cr	18	17	16	11	14	20	15	8	10
Co	9	5	9	2	1	15	<1	<1	<1
Ni	15	11	47	30	37	12	10	11	18
Cu	17	13	10	14	14	11	12	17	10
Zn	87	75	80	54	46	108	71	66	64
Ga	29	23	23	21	19	24	27	28	25
Rb	159	168	205	154	167	260	343	281	301
Sr	1324	1018	825	814	615	791	269	260	331
Y	42	32	32	21	21	35	42	34	37
Zr	413	380	341	287	244	350	148	150	201
Mo	<10	<10	<10	<10	<10	<10	<10	<10	<10
Sn	10.2	15.5	<5	<5	<5	24	<5	<5	<5
Cs	23	27	1	1	<1	36	<1	9	<1
Ba	1743	1637	1000	1289	643	553	273	692	626
La	19	11	19	15	16	29	21	30	19
Eu	1	3	2	2	1	3	1	3	1
Tb	<2	<2	<2	<2	<2	<2	<2	<2	<2
Yb	5	4	3	<1	3	2	2	3	4
Hf	13	11	7	8	8	8	7	8	8
Pb	48	33	27	32	38	25	45	50	43
Th	35	31	26	25	3	36	17	13	21
A/CNK	0.91	1.08	0.95	1.06	1.06	0.96	1.11	1.18	1.22
CIPW normative minerals									
Quartz	3.82	11.09	11.44	12.60	19.22	11.96	17.40	20.21	16.44
Albite	30.97	30.38	29.02	26.74	27.33	28.77	30.55	25.89	24.03
Anorthite	13.43	9.55	13.77	8.82	8.33	16.04	4.76	4.31	3.98
Orthoclase	21.27	21.04	17.20	24.88	19.74	12.53	22.22	23.82	29.08
Corundum	0.00	1.77	0.49	1.34	1.06	0.91	1.62	2.35	2.89
Hypersthene	25.21	22.71	23.65	22.29	21.36	24.75	20.69	20.72	20.77
Diopside	1.44	0.00	0.00	0.00	0.00	0.00	0.00	0.00	0.00
Ilmenite	0.97	0.70	1.14	0.70	0.55	1.44	0.38	0.30	0.46
Magnetite	2.13	2.12	2.15	2.10	2.10	2.16	2.09	2.09	2.09
Apatite	0.76	0.63	1.14	0.53	0.30	1.44	0.30	0.30	0.28

determined for selected samples by sequential wavelength-dispersive X-ray fluorescence (XRF) with a Philips Magix-pro automated spectrometer of the Geological Survey of Iran. The analyses were performed on pressed powdered pellets of rock samples and tabulated in Table 1.

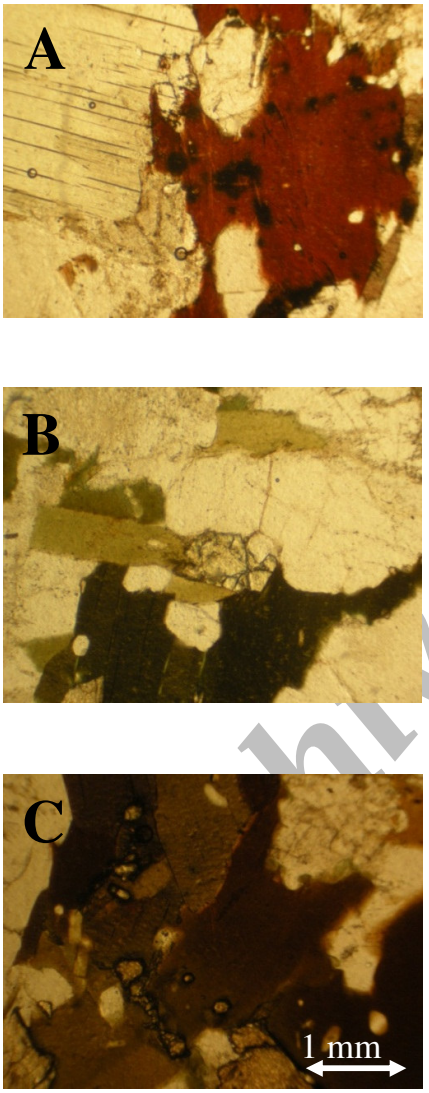

Figure 2. Polarizing microscopic photomicrographs of biotite specimens from Mashhad granitoids. A) Reddish brown biotite in contact with euhedral muscovite in G2 leucogranite. B) green biotite flakes in G1 granodiorite and C) brown biotite flakes in G1 monzogranite. Zircon crystal inclusions characterized by surrounding pleochroic halos. All photomicrographs were taken under plane-polarized light with the same magnification shown by scale bar.

Results and Discussion

In this paper, we use the term 'biotite' in the sense of the IMA classification on Micas [44], i.e., as a series name for true trioctahedral micas between or close to the annite [$(KFe^{2+}{}_3AlSi_3O_{10}(OH)_2$] - phlogopite [$(KMg_3AlSi_3O_{10}(OH)_2$] - siderophyllite [$(KFe^{2+}{}_3AlAl_2Si_2O_{10}(OH)_2$] - eastonite [$(KMg_2AlAl_2Si_2O_{10}(OH)_2$] series.

Biotite Occurrence

Biotite is the main mafic mineral in Mashhad granitic rocks. It occurs as subhedral to euhedral flakes that mostly vary from 0.4 to 5 mm in diameter. It defines a weak to moderate planar fabric in all G1 rock types due to tectonic deformation. Biotite flakes from G1 and G2 granites display a contrast of pleochroism seen in plane polarized light (Fig. 2). In G1 granodiorite and monzogranite samples (Tp 24, Tp-29, Tp-35, Tp-41) biotite is light brown to dark brown pleochroic, in other G1 granodiorite samples (Tp-36, Tp-28) it is light greenish brown to dark greenish brown; biotite from G2 leucogranite (Tp-42, Tp -44, Tp -23,) displays light brown to deep reddish-brown. In addition, apatite and the pleochroic halos surrounding minute zircon inclusions within biotite is the common feature of all samples. Chlorite as an alteration product is rare in the study samples.

Biotite Composition

All 9 mica specimens analyzed are trioctahedral true micas ($5.34 < \Sigma Y$ site < 5.66 atoms per formula unit) that the mean chemical composition of each is presented in Table 2 along with its respective structural formula based on 22 oxygen atoms. Contents of FeO and Fe_2O_3 of the 3 specimens were determined by applying the $Fe^{3+}/(Fe^{2+} + Fe^{3+})$ ratios determined by wet chemistry (WC) as described above. For those samples not measured by WC, the above ratios were extrapolated from those of similar petrographic units.

Polarized light microscopic study shows that biotite has a primary or magmatic origin as it could only be used if secondary phenomena like metamorphic recrystallization, hydrothermal fluids and etc. would not affect its composition. This was further confirmed by Nachit et al. [39] $10TiO_2$ - FeO*(=FeO+MnO) - MgO ternary diagram discriminating magmatic or primary biotite from secondary or re-equilibrated primary one. On this diagram, the biotite samples from both G1 and G2 granites plot in the primary biotite field i.e., the magmatic origin is verified by their composition (Fig. 3). In addition, our study biotite samples have

octahedral Al contents less than 1 (based on 22 oxygen atoms) (Table 2) a sign of being magmatic, as secondary biotites from domains B and C always have a high octahedral Al content, i.e., their octahedral Al contents are larger than [39].

The compositional differences between the G1 and G2 biotite specimens can be distinguished on several points. In all samples of biotite, whether G1 or G2 there is adequate Al to completely fill the tetrahedral sites and there is a surplus of Al carried over to the tetrahedral sites. However, the difference of their total Al contents

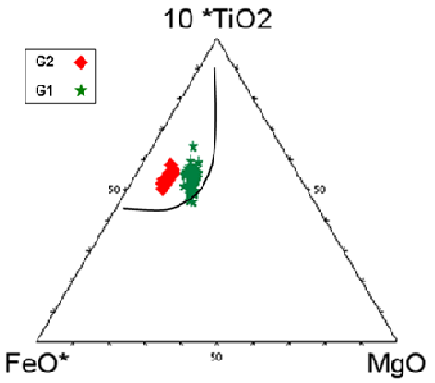

Figure 3. Chemical composition of Mashhad biotites in the $10TiO_2$–FeO*–MgO ternary diagram of Nachit et al. [39] discriminating between primary magmatic, reequilibrated and neoformed biotites. (A) Domain of the primary magmatic biotites, (B) domain of the reequilibrated biotites and (C) domain of the neoformed biotites.

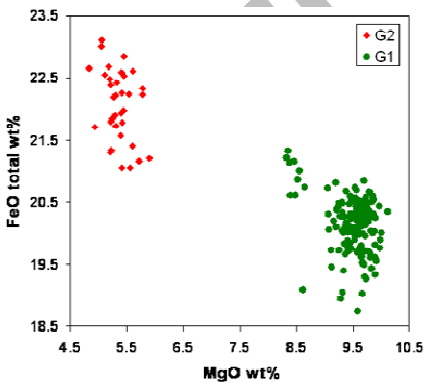

Figure 4. Composition of biotite from Mashhad G1 and G2 granitic rocks plotted in MgO versus FeO total diagram. Note how the biotite from both groups plot separately in this diagram. Mg-rich and Fe-rich biotites are characteristic of G1 and G2 granites, respectively.

makes a distinction between the G1 biotite and the G2. The total Al content of G1 biotite is in the range of 2.8 to 3.1 (apfu), whereas, in G2 in the range of 3.3 to 3.6 (Table 2).

Similarly, in Figure 4 the comparison of MgO with total FeO contents shows that biotite in G1 granites contain more MgO and relatively low Fe/(Fe+Mg) values in the range of 0.52 to 0.59, whereas, biotite in G2 leucogranites contain more FeO and relatively high Fe/(Fe+Mg) of 0.67 to 0.72, i.e., the compositions of biotite in G1 granites are Mg-rich while, those in G2 are Fe-rich.

$Fe^{3+}/(Fe^{2+}+Fe^{3+})$ values, obtained by conventional wet-chemical methods on three specimens of green, brown and red pleochroic colors of biotite separated from granodiorite, monzogranite, and leucogranite are 0.23, 0.18 and 0.10, respectively. Noticeably, $Fe^{3+}/(Fe^{2+}+Fe^{3+})$ values in G1 biotite samples are considerably higher than that of G2 biotite indicating relatively more oxidizing conditions for G1 biotite and more reducing for G2. Karimpour et al. [27] analyzed 12 specimens of biotite from all varieties of Mashhad granitoids (Dehnow tonalite, Vakilabad and Kuhsangi granodiorites, feldspar monzogranite and leucogranite). They determined the Fe_2O_3 and FeO contents of biotite samples based on the Fe_2O_3 and FeO contents of their host rocks determined using titration method. Therefore, the $Fe^{3+}/(Fe^{2+}+Fe^{3+})$ values of their reported biotite data are in the range of 0.29 to 0.35 which are considerably larger.

Biotite from G1 and G2 granites have almost the same TiO_2 contents (Table 2), however, fluorine microprobe determination demonstrates that although biotite in leucogranite shows some overlap in F contents it possesses higher F contents than that of G1 one (Table 2). The higher fluorine content may indicate a relatively high HF/H_2O ratio and low-water fugacity in the source material [31] which is consistent with the reduced nature of G2 rocks.

Oxygen Fugacity Determination

The experimental work of Wones and Eugster [31] clearly established the relationship between biotite composition and oxygen fugacity, thereby making this mineral a valuable indicator of redox conditions in granitic magmas. In Figure 5 the composition of biotite from Mashhad granitoids is plotted in the Fe^{3+}-Fe^{2+}-Mg diagram of Wones and Eugster [57], along with three common oxygen fugacity buffers: quartz-fayalite-magnetite (QFM), nickel-nickel oxide (NNO) and hematite-magnetite (HM). Added to this diagram is the boundary separating magnetite granitoids from ilmenite

Table 2. Electron microprobe analyses of biotite from Mashhad G1 and G2 granitoids along with their respective structural formulae based on 22 oxygen atoms

	G1 granites						G2 granites		
Sample No. mean	Tp-28	Tp-36	Tp-24	Tp-35	Tp-41	Tp-29	Tp-45	Tp-42	Tp-23
of analysis points	56	11	49	12	12	14	12	11	12
SiO_2	36.22	36.32	36.27	35.36	35.65	36.28	35.50	35.36	35.47
TiO_2	2.88	2.47	3.01	3.14	3.40	2.87	2.90	3.03	3.05
Al_2O_3	16.27	16.75	16.38	16.31	16.53	16.77	18.72	19.41	18.93
Fe_2O_3	5.08	5.16	4.01	4.00	4.15	4.02	2.48	2.45	2.43
FeO	15.61	15.55	16.45	16.39	17.00	16.47	20.09	19.80	19.71
MnO	0.59	0.77	0.54	0.67	0.65	0.59	0.88	0.78	0.66
MgO	9.66	9.17	9.59	9.45	8.72	9.59	5.34	5.19	5.54
BaO	0.26	0.20	0.22	0.21	0.14	0.22	0.14	0.14	0.13
CaO	0.07	0.05	0.01	0.01	0.04	0.06	0.01	0.07	0.01
Na_2O	0.08	0.07	0.07	0.08	0.07	0.09	0.07	0.09	0.07
K_2O	9.34	8.78	9.28	9.17	9.09	8.74	9.18	9.21	9.06
F	0.76	0.69	0.90	0.35	0.54	0.54	1.40	1.58	1.05
Cl	0.01	0.02	0.01	0.02	0.01	0.00	0.01	0.00	0.01
total	96.81	96.01	96.74	95.15	96.00	96.22	96.71	97.11	96.12
Mineral formulae based on 22 oxygens									
Si	5.48	5.52	5.50	5.43	5.44	5.49	5.47	5.43	5.46
AlIV	2.52	2.48	2.50	2.57	2.56	2.51	2.53	2.57	2.54
Z site	8.00	8.00	8.00	8.00	8.00	8.00	8.00	8.00	8.00
AlVI	0.38	0.51	0.42	0.39	0.42	0.48	0.87	0.93	0.89
Ti	0.33	0.28	0.34	0.36	0.39	0.33	0.34	0.35	0.35
Fe^{3+}	0.58	0.59	0.46	0.46	0.48	0.46	0.29	0.28	0.28
Fe^{2+}	1.97	1.97	2.09	2.11	2.17	2.08	2.59	2.54	2.54
Mn	0.08	0.10	0.07	0.09	0.08	0.08	0.11	0.10	0.09
Mg	2.18	2.08	2.17	2.16	1.99	2.16	1.23	1.19	1.27
Y site	5.51	5.53	5.54	5.57	5.53	5.59	5.42	5.40	5.42
Ba	0.02	0.01	0.01	0.01	0.01	0.01	0.01	0.01	0.01
Ca	0.01	0.01	0.00	0.00	0.01	0.01	0.00	0.01	0.00
Na	0.02	0.02	0.02	0.02	0.02	0.03	0.02	0.03	0.02
K	1.80	1.70	1.79	1.80	1.77	1.69	1.80	1.80	1.78
X site	1.85	1.73	1.83	1.84	1.81	1.72	1.83	1.84	1.81
F	0.36	0.33	0.43	0.17	0.26	0.26	0.68	0.77	0.51
Cl	0.00	0.01	0.00	0.01	0.01	0.00	0.00	0.00	0.00
Fe/(Fe+Mg)	0.54	0.55	0.54	0.54	0.57	0.54	0.70	0.70	0.69
Al tot	2.90	3.00	2.87	2.95	2.97	2.99	3.40	3.51	3.43

granitoids by Buda et al., [11]. The G1 biotite compositions plot above the NNO buffer whereas, G2 ones fall on the NNO buffer. As it can be seen from the diagram, the G1 biotite specimens fall in the field of magnetite granitoids and G2 ones in ilmenite granitoids; this is consistent with the presence of magnetite and ilmenite in their host rocks. In fact, the presence of Mg-biotite, magnetite, allanite and euhedral titanite in G1 granites of Mashhad are all an indication of relatively oxidizing condition of magma [23,58,10], in contrast, the reducing conditions are inferred in muscovite-biotite leucogranite by the presence of Fe-biotite and ilmenite [23].

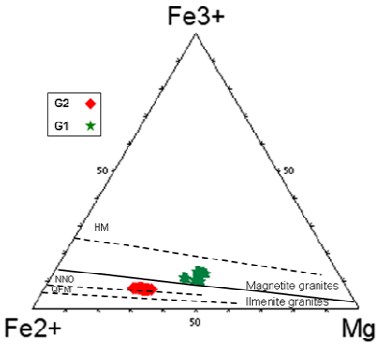

Figure 5. Composition of biotite from Mashhad G1 and G2 granitic rocks plotted in the Fe^{2+}–Fe^{3+}–Mg diagram of Wones and Eugster [57], along with the three common $f(O_2)$ (oxygen fugacity) buffers: quartz – fayalite – magnetite (QFM), nickel – nickel oxide (NNO), and hematite–magnetite (HM). The solid line discriminates magnetite granites realm from ilmenite granites one.

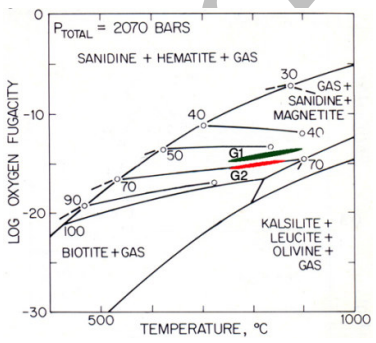

Figure 6. Log $f(O_2)$ – T diagram of Wones and Eugster [57] for the biotite + sanidine + magnetite + gas equilibrium at P_{total} = 2070 bars. Illustrated are Fe/(Fe + Mg) isopleths. Labeled fields represent the range of oxygen fugacity for samples from Mashhad G1 and G2 granitic rocks assuming an equilibrium temperature of 750–900°C.

A qualitative evaluation of oxygen fugacity can also be made from the Fe/(Fe+Mg) ratio of biotite by using the calibrated curve of Wones and Eugster [57] in f (O2)-T space (Fig. 6). Assuming a reasonable range of crystallization temperatures of 750 to 900 °C for these rocks, estimated $f(O2)$ values for G1 granites [Fe/(Fe+Mg) = 0.52-0.59] are between 10^{-12} and 10^{-13} bars corresponding to conditions at or above the NNO buffer. In the same way, biotite from G2 granites [Fe/(Fe+Mg)=0.68-0.72] would have equilibrated at an oxygen fugacity between 10^{-14} and $10^{-15.5}$ bars, close to the QFM buffer.

Composition of Biotite in the ASPE Quadrilateral

The annite - siderophyllite - phlogopite - eastonite quadrilateral (ASPE) is commonly adopted to illustrate the total Al and Fe/(Fe+Mg) compositional relationships of trioctahedral micas from igneous rock suites [50]. This diagram is particularly powerful since these two variables represent, respectively, indicators of peraluminosity and redox state of the rock hosting the mica.

Biotite compositions from G1 and G2 granitic rocks in ASPE quadrilateral occupy two distinct fields defined each by a relatively narrow range of Fe/(Fe+Mg) values but with a relatively large range in total aluminum from 2.8 to 3.1 and 3.3-3.6 atom per formula unit (a.p.f.u), respectively (Fig. 7). In other words, biotite compositions exhibit a trend of increasing total Al contents at relatively constant Fe/(Fe+Mg) values. This trend is relatively common and is observed in biotites of the Adamello massif [14], the Southern Piedmont granites of the Appalachians [49, 51], the Umm Naggat stock of Egypt [26], the Zaer granite of Morocco [34], the granites of Northern Portugal [40], the I-type strongly contaminated reduced granites of the California batholiths [2], the Hepburn intrusive suite of Wopmay orogen [30], and granites of Gander zone of the Canadian Appalachians in New Brunswick [47]. All these suites of granites are believed to have undergone significant Al-enrichment and reduction by assimilation of graphitic metasedimentary wall-rocks during their intrusion (e.g., [30, 2]). In this way, Flood and Shaw [17] suggest the presence of carbon or sulphur in the sedimentary source rocks results in S-types being much more reduced than I-types. For that reason, it seems that such conditions presumably might have been prevailed during biotite crystallization in G2 S-type Mashhad granitoids, i.e., the progressive increase of higher values of total Al in G2 biotite at lower oxygen fugacity during crystallization suggests anatexis of reduced meta-sedimentary material.

The trend defined by G1 biotite characterized with

lower Fe/(Fe+Mg) values may suggest that the granodiorite and monzogranite evolved under slightly more oxidizing conditions and less crustal contribution. This interpretation is consistent with the coexistence of magnetite and euhedral titanite and allanite in these rocks [10,23,58].

Biotite Compositions in Abdel-Rahman's Discrimination Diagram

Abdel-Rahman [1] also introduced several useful diagrams to discriminate the composition of biotite from different tectonic settings, i.e., discriminating between: i) anorogenic extension-related alkaline rocks, ii) calc-alkaline I-type orogenic suites and iii) peraluminous

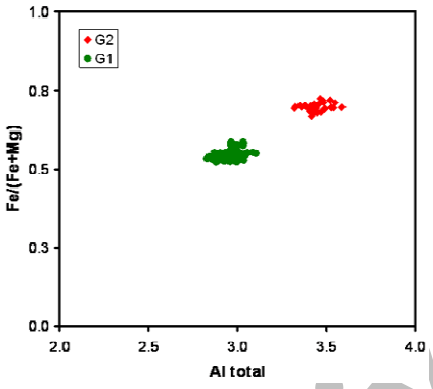

Figure 7. Composition of biotite from Mashhad G1 and G2 granitic rocks plotted in the Fe/(Fe + Mg) versus Al total diagram, also known as the annite– siderophyllite–phlogopite–eastonite (ASPE) quadrilateral [50].

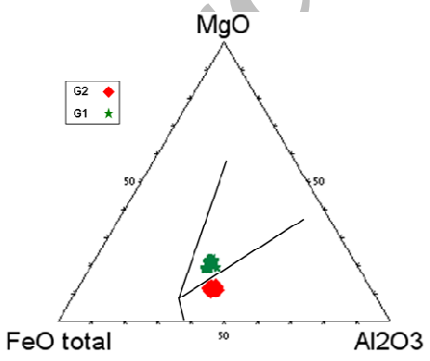

Figure 8. Composition of biotite from Mashhad G1 and G2 granitic rocks plotted in the discrimination diagrams of Abdel-Rahman [1]. A: alkaline, C: calc-alkaline, and P:peraluminous granite fields. FeO* = [FeO + (0.89981*Fe2O3)].

rocks including S-type granites. This indicates that biotite compositions largely depend upon the nature of host magmas. Of all his diagrams, the ternary FeO*-MgO-Al_2O_3 plot is probably the most powerful discriminant since, much like the ASPE quadrilateral; it reflects variations in redox state and peraluminosity. In the ternary FeO*-MgO-Al_2O_3 diagram of Abdel-Rahman [1], biotite compositions from G2 rocks plot in peraluminous field indicating S-type nature of granite, derived by melting of crustal source in a collisional environment and those of G1 plot in calc-alkaline orogenic I-type field (Fig. 8).

In conclusion, biotite composition in granitic rocks could be used as a powerful tool to investigate their parental magma. It is also useful to separate different granitic suits based on their biotites. In the case of Mashhad granites in NW of Iran, based on biotite chemistry, two groups can be distinguished, Mg-rich and Fe-rich biotite corresponding to two phases of granitoids, G1 and G2. Mg-rich biotite, showing brown to greenish brown pleochroic colors in plane polarized light, occurs in G1 weakly peraluminous and relatively oxidized I-type granites, whereas, reddish brown Fe-rich biotite appears in G2 moderately peraluminous and reduced S-type granites. The distinctive compositional differences between the two groups of biotite can be considered as different crystallization conditions, protoliths, geodynamics and etc.

Acknowledgments

Marcello Serracino is thanked for skillful help during microprobe analyses. N. Amiri, and A. Abolhassani, from Geological Survey of Iran, are also thanked for wet chemistry and XRF analyses.

References

1. Abdel-Rahman A. M. Nature of biotites from alkaline, calc-alkaline and peraluminous magmas. J. Petrol., **35**, 525-541 (1994).
2. Ague J.J. and Brimhall G. H. Regional variations in bulk chemistry, mineralogy and the compositions of mafic and accessory minerals in the batholiths of California. Geol. Soc. Am., Bull. **100**, 891-911 (1988).
3. Alavi M. Sedimentary and structural characteristics of the Paleo-Tethys remnants in northeastern Iran. Geol. Soc. Am. Bull., **103**, 983-92 (1991).
4. Alavi M. Thrust tectonics of the Binalood region, NE Iran. Tectonics, **11**(2), 360-70 (1992).
5. Alberti A. and Moazez Z. Plutonic and metamorphic rocks of the Mashhad area (NE Iran, Khorasan). Bull. Soc. Geol. Italy, **93**, 1157-1196 (1974).
6. Aydin F., Karsli O., and Sadiklar M. B. Mineralogy and Chemistry of Biotites from Eastern Pontide Granitoid

Rocks, NE-Turkey: Some Petrological Implications for Granitoid Magmas**.** Chemie der Erde, **63**, 163-182 (2003).
7. Barzegar H. Relationship between biotite composition and tectonomagmatic affinity of the granodiorite intrusion at the Seridune prospect, Iran. International Geological Congress, Oslo, 2008, August 6th-14th.
8. Bónová K., Broska I., Lipka J. and Tóth I. Composition of biotites from Čierna Hora granitoids (Western Carpathians) as an indicator of the granite tectonic setting. Geolines, vol. **20** (2006).
9. Bónová K., Broska I. and Igor P. Biotite from Čierna hora Mountains granitoids (Western Carpathians, Slovakia) and estimation of water contents in granitoid melts. Geologica Carpathica, 1335-0552 (print) (2010).
10. Broska I. REE accessory minerals in the felsic silicic rocks of the west-carpathians: their distribution, composition and stability. Acta Mineralogica-Petrographica, Abstract Series 1, Szeged, 2003.
11. Buda G., Koller F., Kovács J. Jaromír and Ulrych J. Compositional variation of biotite from Variscan granitoids in Central Europe: A statistical evaluation. Acta Mineralogica-Petrographica, Szeged, vol. **45/1**, 21-37 (2004).
12. Burkhard D. J. M. Biotite crystallization temperatures and redox states in granitic rocks as indicator for tectonic setting. Geol. Mijnbouw **71**, 337-349 (1993).
13. Chappell B. W. and White A. J. R. Two contrasting granite types. Pacific Geol., **8**, 173-4 (1974).
14. De Pieri R. and Jobstraibizer P. G. On some biotites from Adamello massif, northern Italy. Neues Jahrbuch für Mineralogie Monatshefte, 15-24 (1977).
15. Didar P. Geochemistry of Mashhad granitoids with a special approach to REE. M.Sc. thesis (in Farsi), Research Center for Earth Sciences, Geological Survey of Iran, (2004).
16. Esmaeily D. and Maghdour-Mashhour R. Geochemistry of biotites from Boroujerd granitoid complex, SSZ, Iran: A crucial factor for illustration petrogenesis and tectonomagmatic environment of host rock? Geophysical Research Abstracts, vol. **11**, EGU2009-7980 (2009).
17. Flood R. H. and Shaw S. E. A Cordierite bearing granite suite from the New England Batholith". Contr. Mineral. & Petrol., vol. **52**, pp.157-164 (1975).
18. Ghani A. A. Geochemistry of biotite from Kuala Lumpur Granite. Malaysian Journal of Science, **21** (1 and 2), 159-164 (2002).
19. Hasaniepak A. A., Ghazi, A. M., Mobasher K., Tucker, P. J., and Duncan R. A., 40Ar-39Ar geochronology and geochemistry of the Paleo-Tethyan Mashhad ophiolite, N.E. Iran, Tectonophysics, **7/35**, 173-196 (2004).
20. Hecht L. The chemical composition of biotite as an indicator of magmatic fractionation and metasomatism in Sn-specialised granites of the Fichtelgebirge (NW Bohemian massif, Germany). In: R. Seltmann, H. Kämpf and P. Möller (Editors), Metallogeny of collisional orogens. Czech Geol. Survey, Prague, 295-300 (1994).
21. Helmy H. M., Ahmed A. F., El Mahallawi M. M., and Ali S. M. Pressure, temperature and oxygen fugacity conditions of calc-alkaline granitoids, Eastern Desert of Egypt and tectonic implications, Journal of African Earth Sciences, **38**, 255-268 (2004).
22. Iranmanesh J. and Sethna S. F. Petrography and geochemistry of the Mesozoic granites at Mashhad, Khorasan Province, NE Iran. Journal of the Geological Society of India, **52**(1):87-94 (1998).
23. Ishihara S. The magnetite-series and ilmenite-series granitic rocks. Mining Geol. **27**, 293-305 (1977).
24. Ishihara S. The granitoid series and mineralization. Econ. Geol., 75th Anniv. vol., 458-484 (1981).
25. Jiang Y., Jiang S., Ling H., Zhou X., Rui X., and Yang W. Petrology and geochemistry of shoshonitic plutons from the western Kunlun orogenic belt, Xinjiang, northwestern China: implications for granitoid geneses. Lithos, **63**, 165-187 (2002).
26. Kabesh M. L., Aly M. M., and Refaat A. M. On the chemistry of biotites and variation of ferrous/ferric ratios in granitic rocks of Umm Naggat stock, Egypt. Neues Jahrbuch fur Mineralogie Abhandlungen, **124**, 47-60 (1975).
27. Karimpour M. H., Farmer L., Ashouri C., and Saadat S. Major, Trace and REE geochemistry of Paleo-Tethys Collision-Related Granitoids from Mashhad, Iran. Journal of Sciences, Islamic Republic of Iran **17**(2): 127-145 (2006).
28. Karimpour M. H., Farmer G. L., Stern C. R. Geochronology, radiogenic isotope geochemistry and petrogenesis of Sangbast Paleo-Tethys monzogranite, Mashhad, Iran. Iranian Society of Crystallography and Mineralogy, **17**, no. 4, 1-14 (2009).
29. Kumar S., Singh B., Joshi C. and Pandey A. Magnetic susceptibility and biotite composition of granitoids of Amritpur and adjoining regions, Kumaun Lesser Himalaya. Extended Abstracts: 19th Himalaya-Karakoram-Tibet Workshop, Niseko, Japan (2004).
30. Lalonde A. and Bernard P. Composition and color of biotite from granites: Two useful properties in the characterization of plutonic suites from the Hepburn internal zone of Wopmay orogen, NW Territories. Canadian Mineralogist, **31**, 203-217 (1993).
31. Li, z., Tainosho Y, Shiraishi K. and Owada M. Chemical characteristics of fluorine-bearing biotite of early Paleozoic plutonic rocks from the Sør Rondane Mountains, East Antarctica, Geochemical Journal, vol. **37**, 145 to 161 (2003).
32. Lima S. S. M., Neiva A. M. R. and Ramos J. M. F. Geochemistry of biotites from granitic rocks of Ciborro – Aldeia da Serra, Ossa-Morena Zone (southern Portugal). Goldschmidt Conference Abstracts 2009, A765 (2009).
33. Machev P. Klain, L. and Hecht, L. Mineralogy and chemistry of biotites from the Belogradchik pluton- some petrological implications for granitoid magmatism in northwest Bulgaria. Bulgarian Geological Society, Annual Scientific Conference "Geology 2004", 16 – 17.12.2004 (2004).
34. Mahmood A. Chemistry of biotites from a zoned granitic pluton in Morocco. Mineralogical Magazine, vol. **47**, PP. 365-9 (1983).
35. Majidi B. Etude petrostructural de la region de Mashhad (Iran). Les problems des metamorphites, serpentinites et granitoides hercyniens. France, these universite Scientifique et Medicale de Granoble (1978).
36. Masoudi F., and Jamshidi-Badr M. Biotite and Hornblende

composition used to investigate the nature and thermobarometry of Pichagchi Pluton, northwest Sanandaj-Sirjan Metamorphic Belt, Iran. Journal of Sciences, Islamic Republic of Iran **19**(4), 1016-1104 (2008).
37. Mirnejad H. Geochemistry and petrography of Mashhad granites and pegmatites, M.Sc. thesis (in Farsi), Tehran University (1991).
38. Nachit H., Razafimahefa N., Stussi J.M. and Carron J. P. Composition chimiques des biotite et typologie magmatique des granitoids. C R Acad. Sci. **301,** 813-818 (1985).
39. Nachit H., Ibhi A., Abia E. H. and Ben Ohod M. Discrimination between primary magmatic biotites, re-equilibrated biotites and neoformed biotites. Geoscience, **337**, 1415-1420 (2005).
40. Neiva A. M. R. The geochemistry of biotites from granites of northern Portugal with special reference to their tin content. Mineralogical Magazine, **40**, 453-466 (1976).
41. Nockolds S. R. The relation between chemical composition and paragenesis in the biotite micas of igneous rocks. American Journal of Science, **245**, 401-420 (1947).
42. Plimer I. R. and Moazez Lesco Z. Garnet xenocrysts in the Mashhad granite, NE Iran. Geologische Rundschau, **69** (3), 801-810 (1980).
43. Pouchou J. L. and Pichour F. A new model for quantitative X-ray microanalysis. Part I Application to the analysis of homogeneous samples. Recherche Aerospatiale, **3**, 167-192 (1984).
44. Rieder M., Cavazzini G., D'Yakonov Y. S., Frank-Kamenetskii V. A. Gottardi G., Guggenheim S., Koval P. V., Muller G., Neiva A. M. R., Radoslovich E. W., Robert J. L., Sassi F. P., Takeda H., Weiss Z. and Wones D. R. Nomenclature of the micas. Canadian Mineralogists, **36**, 905-912. (1998).
45. Sallet R. Fluorine as a tool in the petrogenesis of quartz-bearing magmatic associations: applications of an improved F–OH biotite–apatite thermometer grid. Lithos, **50**, 241-253 (2000).
46. Shabani A. A. T. Lalonde A. E. and Whalen J. B. Composition of biotite from granitic rocks of the Canadian Appalachian: A potential tectonomagmatic indicator? The Canadian Mineralogist, **41**, 1381-1396 (2003).
47. Shabani A. A. T. A comparison of spectroscopic and wet analytical chemistry determinations of iron cations in biotite mineral (in Farsi). 26th Symposium of Geosciences, Geological Survey of Iran proceeding (2006).
48. Shahrabi M. Geodynamic features of the north of Khorasan with a special approach to Binaloud and Kope Dagh Mountains in the Mashhad quadrangle geological map (in Farsi). 18th Symposium on Geosciences, Geological Survey of Iran, vol. **1**, 47-50 (1999).
49. Speer J. A. Petrology of cordierite- and almandine-bearing granitoid plutons of the southern Appalachian Piedmont, U.S.A. The Canadian Mineralogist, **19**; no. 1; p. 35-46 (1981).
50. Speer J. A. Micas in igneous rocks. In: Micas, Bailey, S. W. (editor) Mineralogical Socity of America, Reviews in Mineralogy, **13**, 299-356 (1984).
51. Speer J. A. Evolution of magmatic AFM mineral assemblages in granitoid rocks: The hornblende + melt = biotite reaction in the Liberty Hill pluton, South Carolina, American Mineralogist, **72**, 863-878 (1987).
52. Stone M., Klominsky J., and Rajpoot G. S. Composition of trioctahedral micas in the Karlovy Vary pluton, Czech Republic and a comparison with those in the Cornubian Batholith, SW England. Mineralogical Magazine; December 1997; **61**; no. 6, 791-807 (1997).
53. Stone M. Petrogenetic implications from biotite compositional variations in the Cornubian granite batholith. Mineralogical Magazine; August 2000; **64**, no. 4, 729-735 (2000).
54. Taheri J. and Ghaemi F. Geological map of Mashhad, 1:100000, Geological Survey of Iran (1999).
55. Tarokh A. Geochemistry and petrology of granites and pegmatites in the south of Mashhad with an approach to mineralogy and associated fluids. M.Sc. thesis (in Farsi), Tehran Tarbiat Moallem University (2009).
56. Valizadeh M. V. and Karimpour M. H. Petrogenesis of Mashhad granites and granodiorites and their tectonic setting (in Farsi). No. **1**, 71-82 (1995).
57. Wones D. R. and Eugster H.P. Stability of biotite: experiment, theory, and application. American Mineralogist, **50**, 1228-1272 (1965).
58. Wones D. R. Significance of the assemblage titanite + magnetite + quartz in granitic rocks. American Mineralogist, **74**, 744-749 (1989).